SUPPORTING INFORMATION

for

Interaction of a porphyrinic cage with ethionamide: a spectroscopic and computational study

Federica Ruani,[a] Sonia Adrouche,[b] Gianluca Dell'Orletta,[c] Daniel Sánchez-Resa,[a] Andrea Barbieri,[a] Stéphanie Durot,[b] Isabella Daidone,*[c] Valérie Heitz,*[b] Nicola Armaroli[a] and Barbara Ventura*[a]

[a] Istituto per la Sintesi Organica e la Fotoreattività (ISOF) – Consiglio Nazionale delle Ricerche (CNR), Via P. Gobetti 101, 40129 Bologna, Italy.
[b] Laboratoire de Synthèse des Assemblages Moléculaires Multifonctionnels, Institut de Chimie de Strasbourg, CNRS/UMR 7177, Université de Strasbourg, 4 rue Blaise Pascal, 67000 Strasbourg, France.
[c] Dipartimento di Scienze Fisiche e Chimiche, Università degli Studi dell'Aquila, via Vetoio (Coppito 1), 67100 L'Aquila, Italy.

Table of contents

1. Synthesis and characterization

All chemicals were of the best commercially available grade and used without further purification. NaBArF was purchased from abcr and tetrabutylammonium hexafluorophosphate ($TBAPF_6$, +99%) from Sigma Aldrich. CH_2Cl_2 was distilled over CaH_2 before use.

NMR spectra for ^1H were recorded on Bruker Avance 400, 500 and 600 MHz spectrometers. NOESY and ^{13}C spectra were acquired on a Bruker Avance 500 spectrometer. The ^1H and ^{13}C spectra were referenced to residual solvent peaks (CD_2Cl_2, 5.32 ppm and 53.84 ppm). Coupling constants (J) are reported in hertz (Hz). Standard abbreviations indicating the multiplicity were used as follows: q = quartet, t = triplet, d = doublet, s = singlet, br = broad.

Measurement of self-diffusion coefficients were performed on a BRUKER 600 MHz spectrometer - Avance III, equipped with a BBI probe developing a pulsed field gradient of 50 G/cm. Diffusion NMR data were acquired using a stimulated echo pulse sequence with bipolar z gradients. Limited Eddy current delay was fixed to 5 ms. A recycling delay of 5 s was respected between scans. Experiments were recorded at 298K. The gradient strength varied linearly in 32 or 34 experiments. The diffusion time was set to 150 ms and the duration of the smoothed square gradients to 1500 or 1400 μs. DOSY spectra were generated with Bruker's Dynamic center software using 3 components for exponential fitting.

High-resolution electrospray ionization mass spectrometry (HR ESI-MS) was carried out on a Bruker MicroTOF spectrometer at the mass spectrometry service at the University of Strasbourg.

Synthesis of $[Na_4(1)](BArF)_4$.

To a suspension of cage **1** (2.0 mg, 0.9 μmol, 1 equiv.) in CH_2Cl_2, was added NaBArF (3.19 mg, 3.6 μmol, 4 equiv.). The solution obtained after 2 min of sonication was evaporated under reduced pression to give a purple solid. The residue was dissolved in CD_2Cl_2 for characterization.

^{1}H NMR (400 MHz, CD_2Cl_2, 298 K) δ (ppm): 8.48 (s, 16H, H_{pyr}), 8.06 (d, ^3J = 7.7 Hz, 8H, $H_{o\mathit{out}}$), 7.75 (br s, 32H, $H_{o\text{-}BArF}$), 7.73 (br s, 8H, H_t), 7,70 – 7.61 (m, 16H, $H_{m\mathit{out},o\mathit{in}}$), 7.57 (br s, 16H, $H_{p\text{-}BArF\text{-}}$), 7.22 (d, ^3J = 7.7 Hz, 8H, $H_{m\mathit{in}}$), 5.80 (s, 16H, H_{H1}), 4.74 (s, 16H, H_{H2}), 3.82 (s, 16H, H_{H3}), – 3.50 (s, 4H, H_{NH}). **^{13}C{^{1}H} NMR (126 MHz, CD_2Cl_2, 298K) δ (ppm):** 162.2, 145.2, 142.6, 135.5, 135.2, 135.0, 134.7, 129.3, 126.5, 125.5, 125.0, 121.8, 119.4, 117.9, 69.7, 64.7, 54.6.

HR ESI-MS: m/z = 578.2177 **$[M\text{-}4BArF]^{4+}$**; calcd for $C_{128}H_{108}N_{32}Na_4O_8$ 578.2149; m/z = 794.2364 **$[M\text{-}3BArF+H]^{4+}$** calcd for $C_{160}H_{121}BF_{24}N_{32}Na_4O_8$ 794.2331; m/z = 1058.6457 **$[M\text{-}3BArF]^{3+}$**, calcd for $C_{160}H_{120}BF_{24}N_{32}Na_4O_8$ 1058.6417.

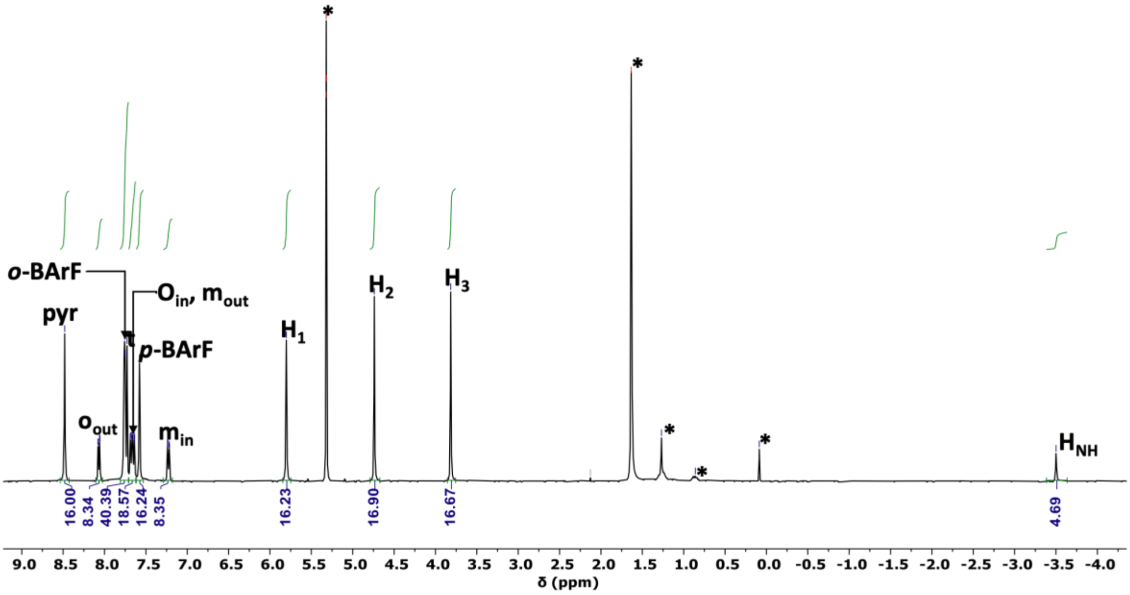

Fig S1. ^{1}H NMR (400 MHz, CD_2Cl_2, 298 K) spectrum of $[Na_4(\mathbf{1})](BArF)_4$. *: residual solvents and grease.

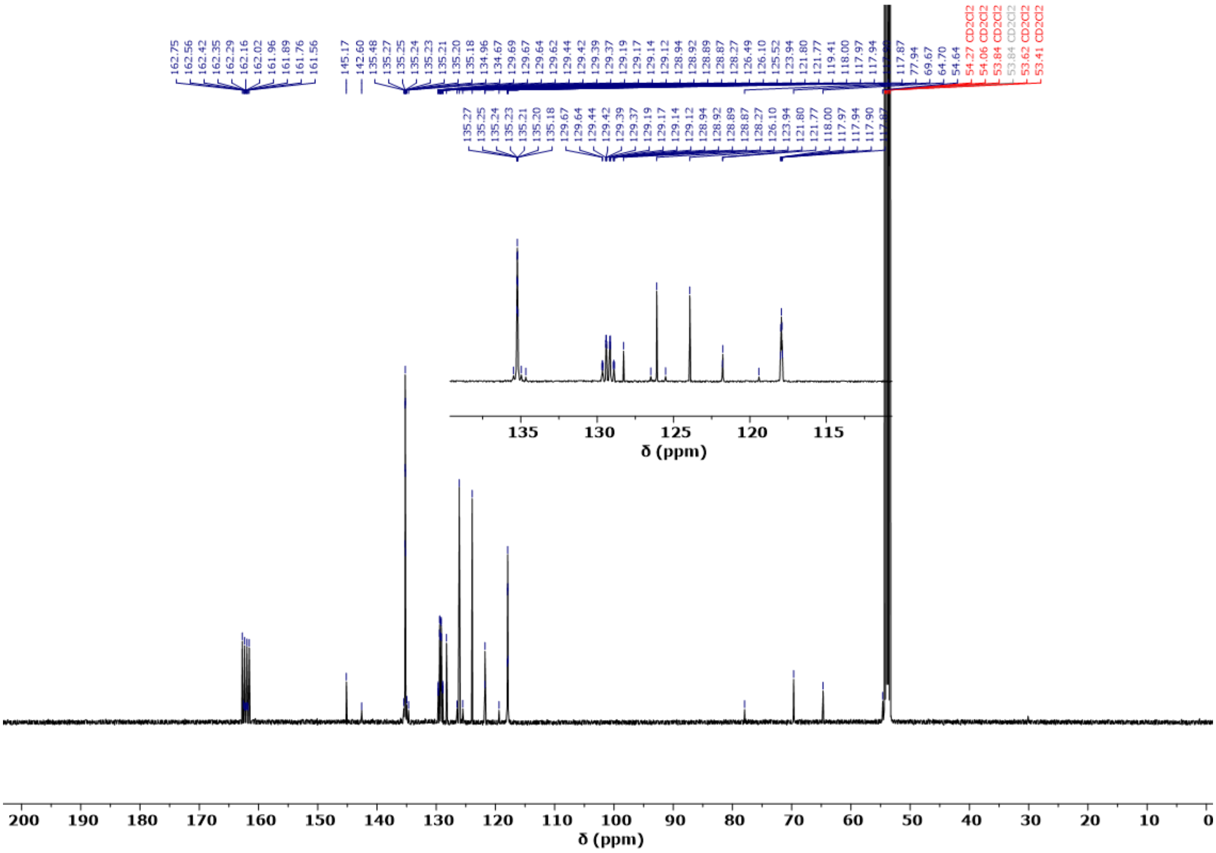

Fig. S2: $^{13}C\{1H\}$ NMR (126 MHz, CD_2Cl_2, 298 K) spectrum of $[Na_4(\mathbf{1})](BArF)_4$.

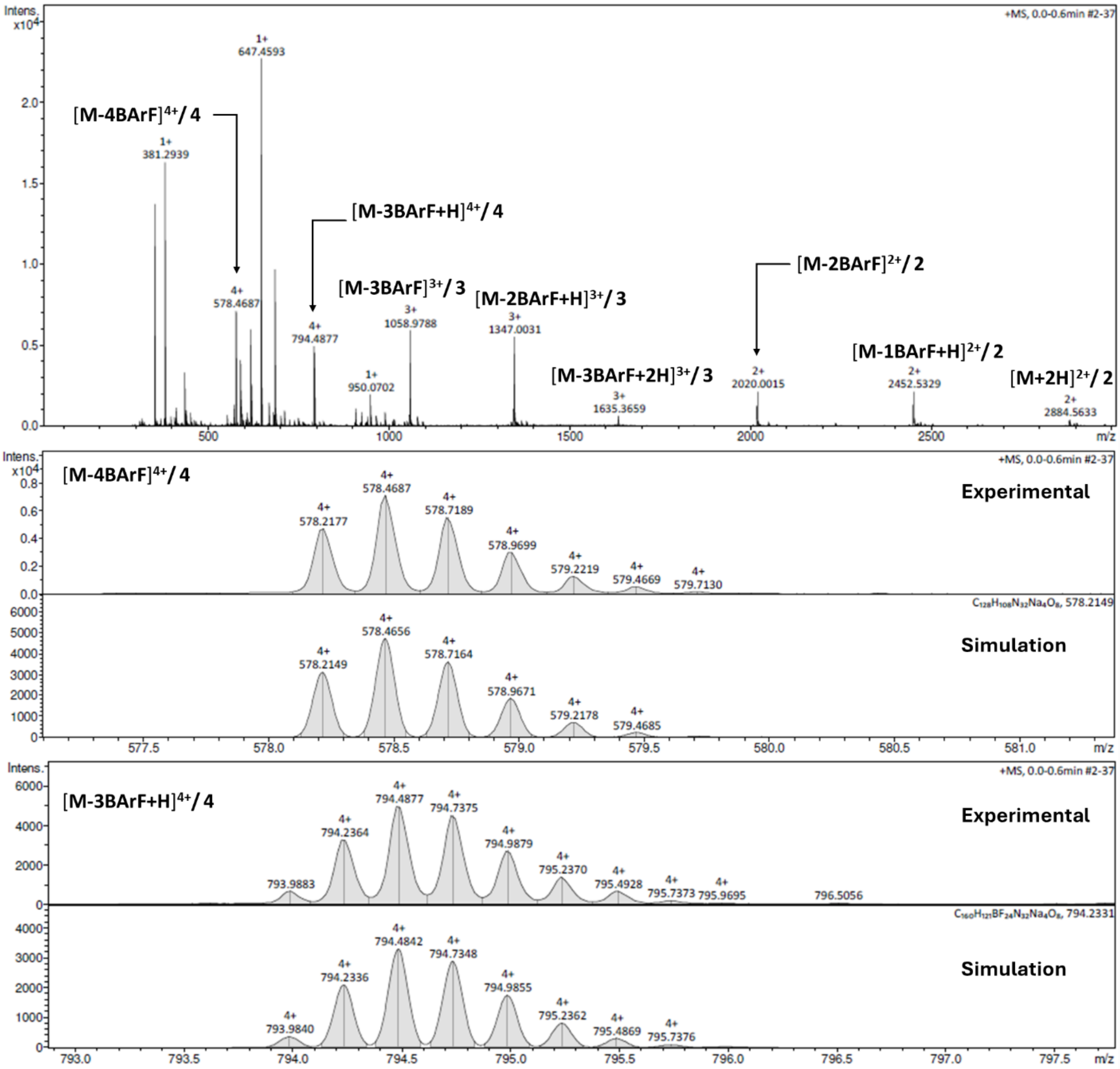

Fig. S3: HR ESI-MS spectrum of $[Na_4(\mathbf{1})](BArF)_4$ and isotopic profiles of the detected cage ions.

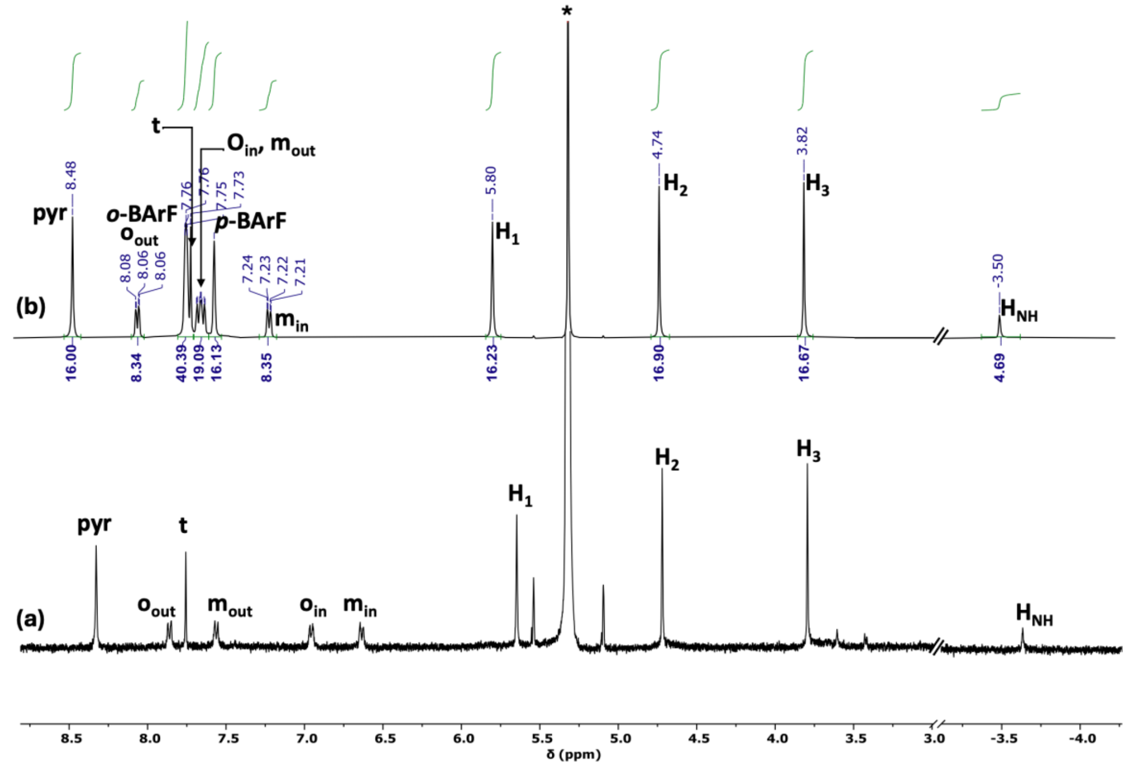

Fig. S4: ^{1}H NMR (400 MHz, CD_2Cl_2, 298 K) spectra of **1** (a), [Na_4(**1**)]$(BArF)_4$ (b). *: residual solvents.

2. Photophysical and electrochemical studies

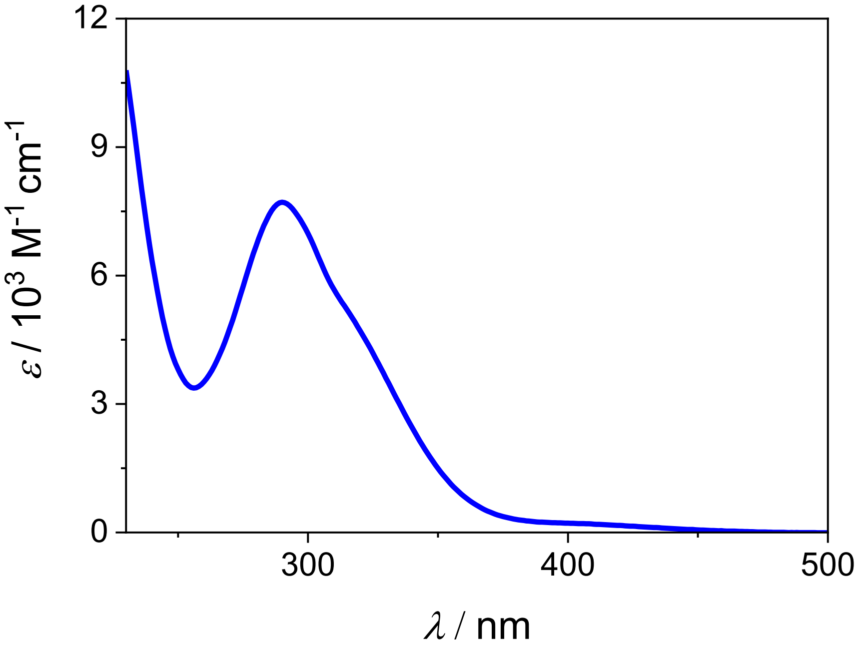

Fig. S5: Absorption spectrum of ETH in CH_2Cl_2:MeOH (9:1).

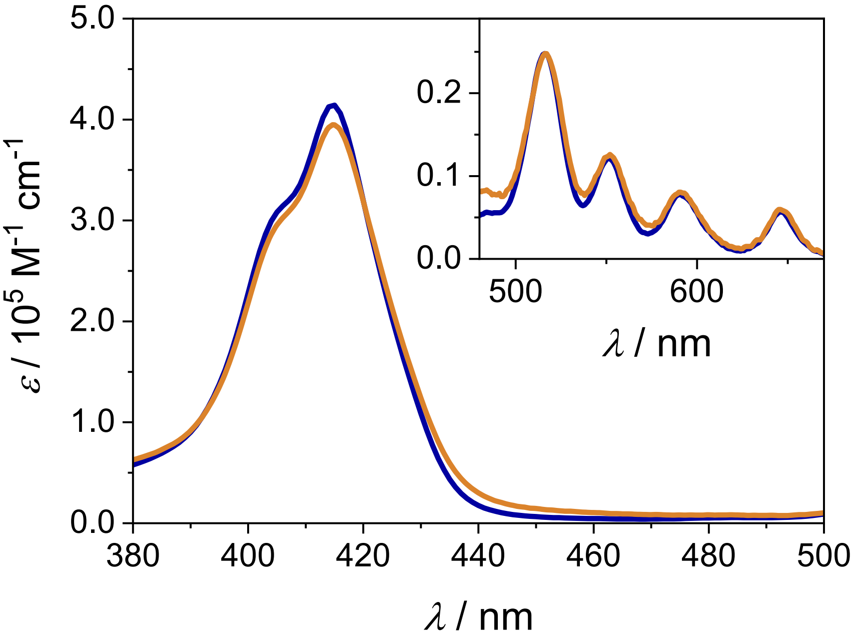

Fig. S6: Comparison between the molar absorption coefficient of the species that is formed at the end of the titration of [Ag_4(**1**)](OTf)$_4$ with ETH (orange), as described in the main text, and that of the closed cage **1** (blue) in CH_2Cl_2:MeOH (9:1). Inset: amplification of the Q-bands region (480-670 nm).

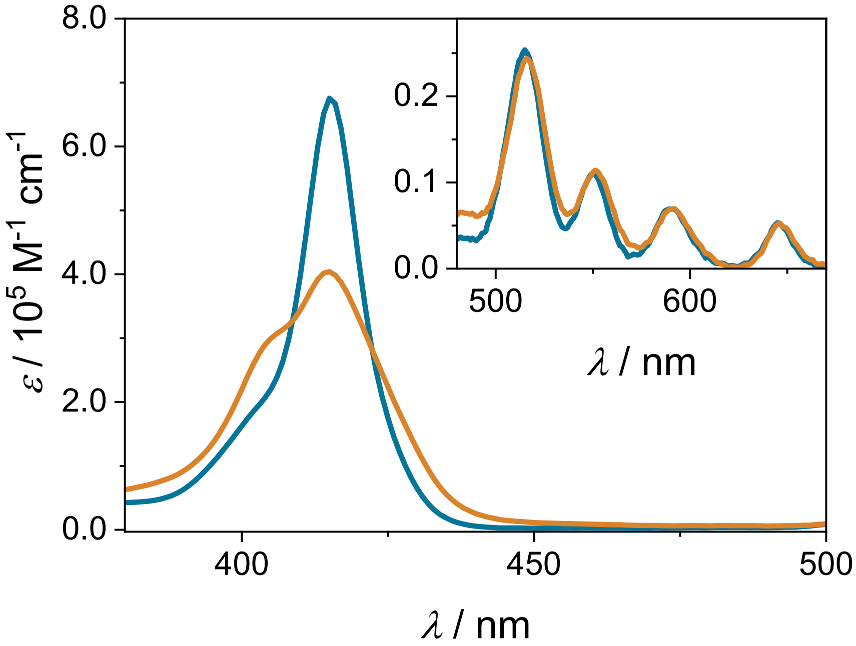

Fig. S7: Simulated absorption spectrum of $[Ag_4(\mathbf{1})](OTf)_4$ interacting with two ETH molecules (orange) compared with the absorption spectrum of $[Ag_4(\mathbf{1})](OTf)_4$ (cyan, fixed in the analysis) in CH_2Cl_2:MeOH (9:1). The fitting was performed with the software Reactlab Equilibria by using a 1:2 ($[Ag_4(\mathbf{1})](OTf)_4$**:**ETH) binding model. Inset: amplification of the Q-bands region (480-670 nm).

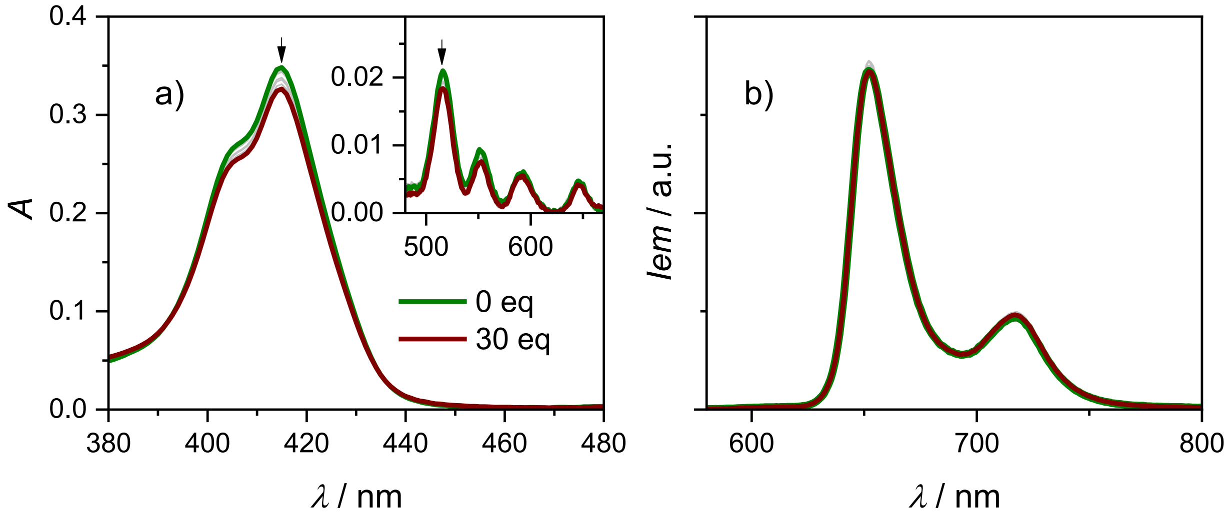

Fig. S8: Absorption (a) and uncorrected emission spectra (λ_{exc} = 390 nm) (b) of solutions in CH_2Cl_2:MeOH (9:1) containing **1** (8.4×10^{-7} M) and increasing amounts of ETH [0-30 equivalents].

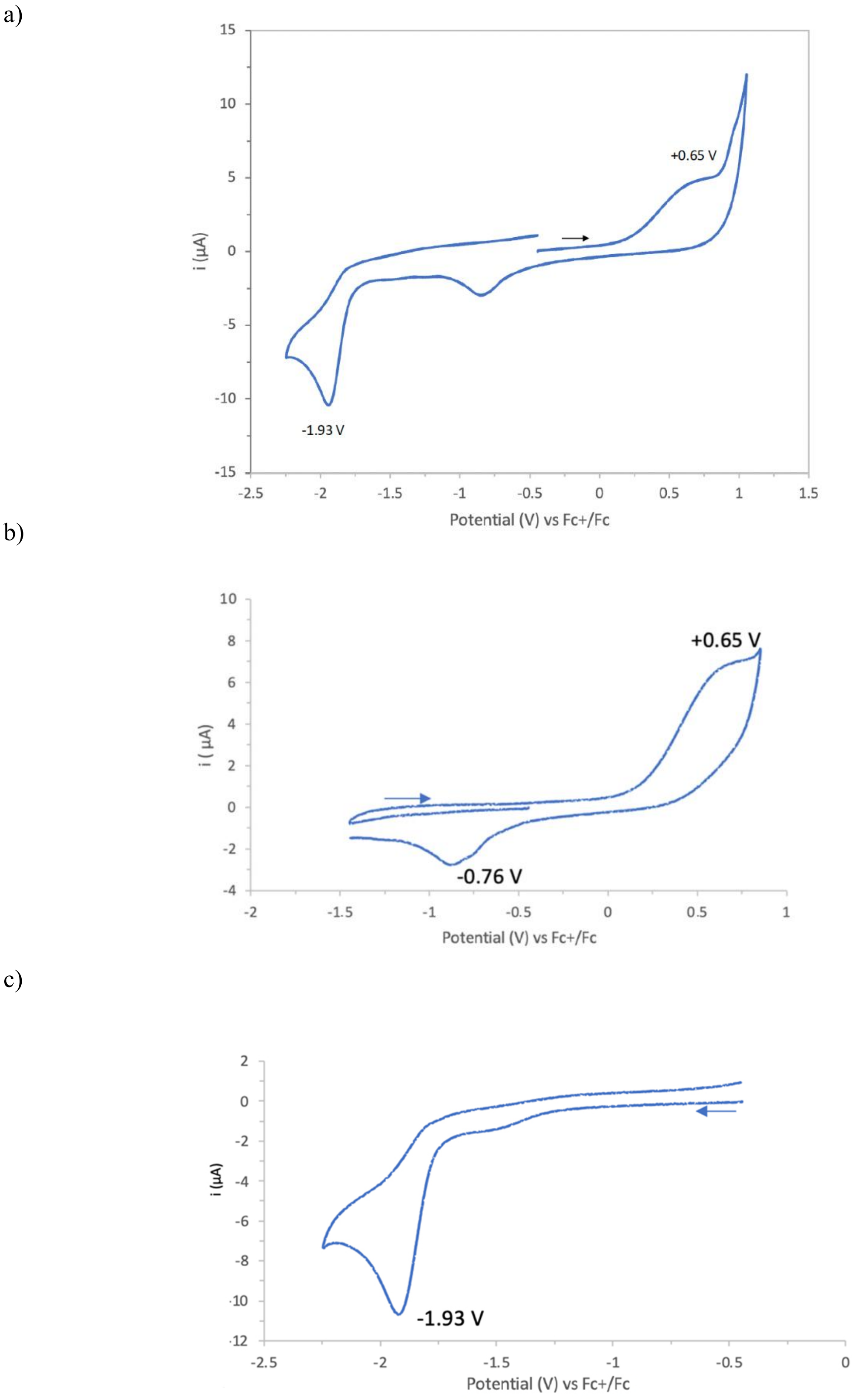

Fig. S9: Cyclic voltammograms (a-c) of ETH in $C_2H_4Cl_2$ at 298 K recorded over different potential ranges. Working electrode: Pt, reference electrode: Ag/AgCl, counter electrode: Pt coil, supporting electrolyte: 0.1 M tetrabutylammonium hexafluorophosphate, scan rate: 100 mV.s^{-1}.

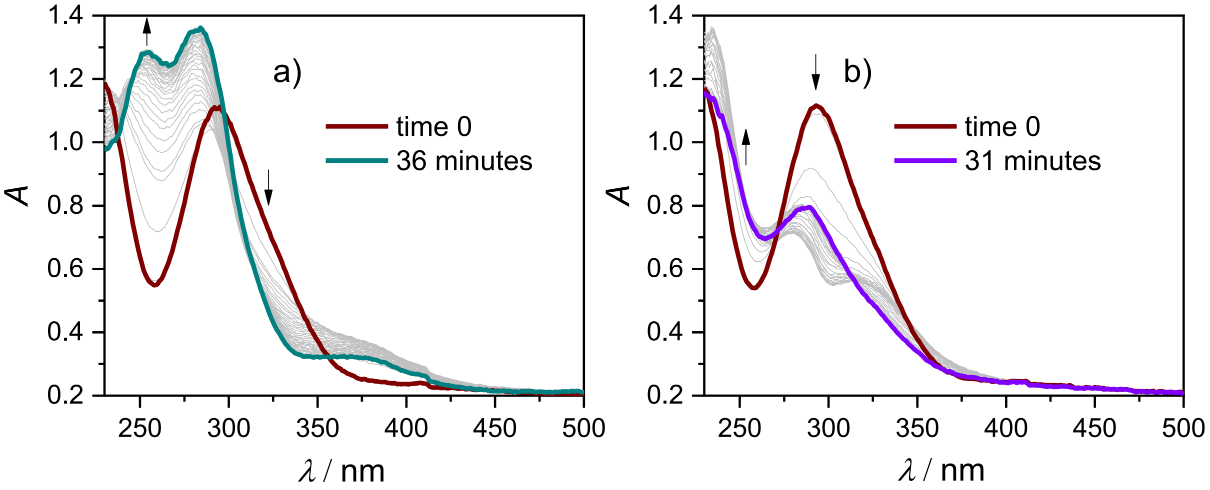

Fig. S10: Spectral variations of solutions 1.1 × 10^{-4} M of ETH under a voltage of 1.44 V (a) and – 2.0 V (b) in CH_2Cl_2 as a function of the time passed after application of the indicate voltage. Working electrode: platinum gauze; reference electrode: Ag/$AgNO_3$ 0.01M in CH_3CN; counter electrode: Pt wire.

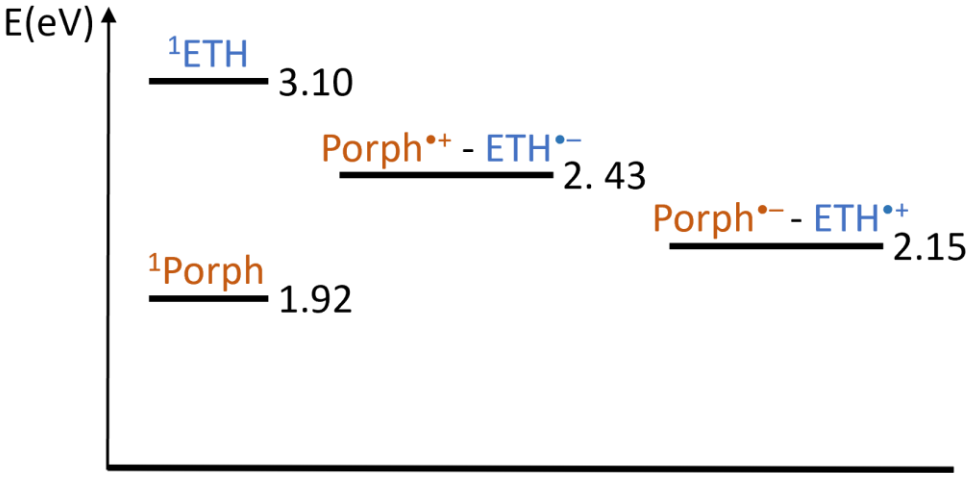

Fig. S11: Energy level diagram for the cage interacting with ETH in CH_2Cl_2. The singlet energy levels are taken from data of the present paper. The energy levels of the charge separated states have been calculated from the redox potentials of the involved species (see main text).

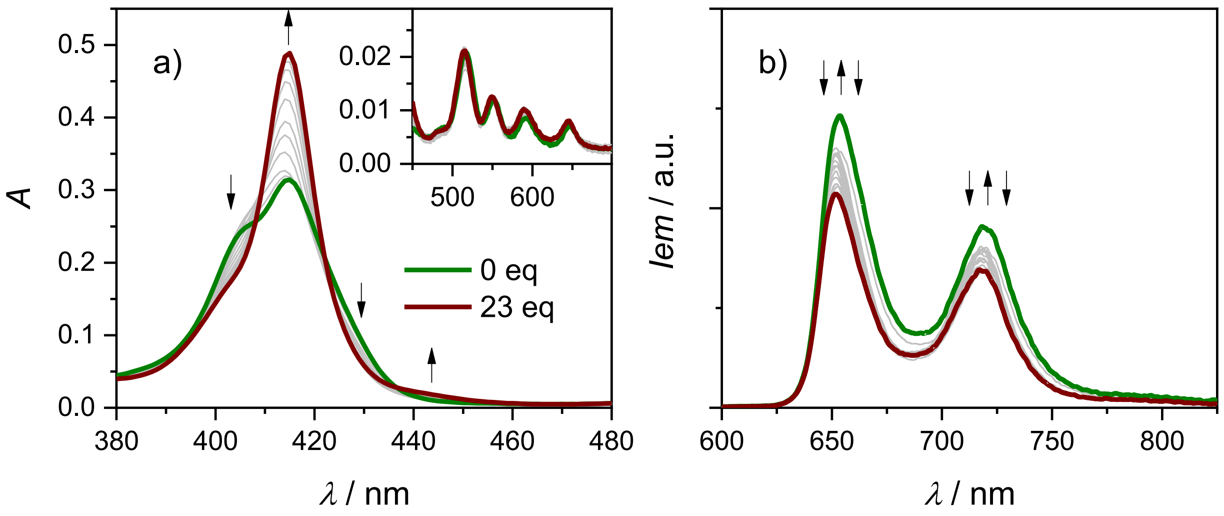

Fig. S12: Absorption (a) and corrected emission spectra (λ_{exc} = 422 nm) (b) of solutions in CH_2Cl_2 containing **1** (6.8×10^{-7} M) and increasing amounts of NaBArF [0-23 equivalents].

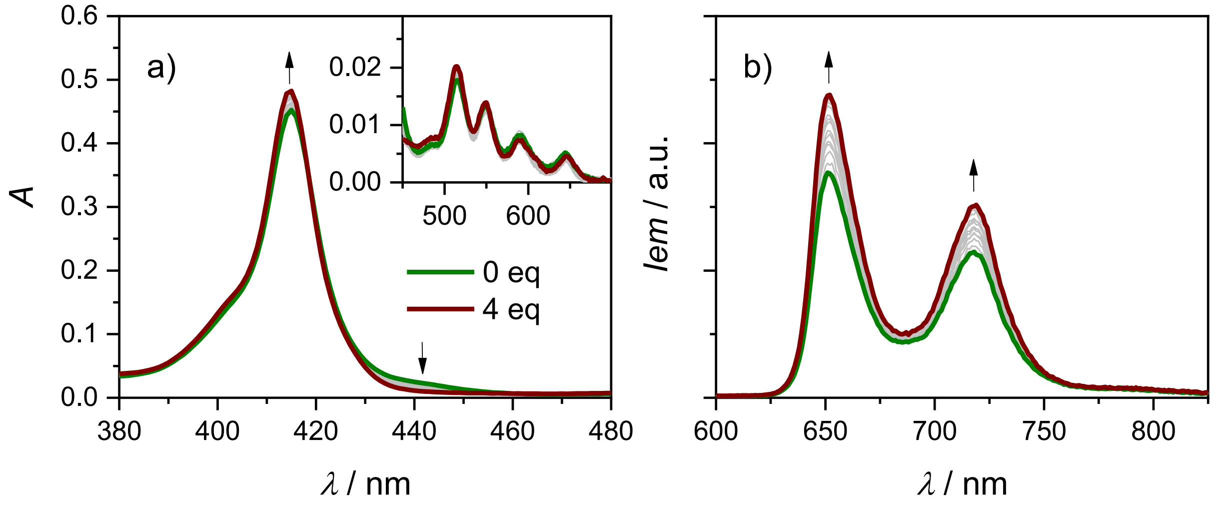

Fig. S13: Absorption (a) and corrected emission spectra (λ_{exc} = 422 nm) (b) of solutions in CH_2Cl_2 containing $[Na_4(\mathbf{1})](BArF)_4$ (5.8×10^{-7} M) and increasing amounts of ETH [0-4 equivalents].

3. NMR studies of ETH interaction with $[Ag_4(\mathbf{1})](BArF)_4$ or $[Na_4(\mathbf{1})](BArF)_4$

3.1 Studies of ETH interaction with $[Ag_4(\mathbf{1})](BArF)_4$

To a solution of cage $[Ag_4(\mathbf{1})](BArF)_4$ (1.83 mg, 0.3 µmol, 1 equiv.) in CH_2Cl_2 was added ETH (of a 3 mM solution in CH_2Cl_2/MeOH (9:1), 7.48 µmol, 1 equiv.) and K_2CO_3 (4 mg, 22 µmol)). The residue was dissolved in 0.6 mL of CD_2Cl_2. Incremental addition of 100 µL of the ETH stock solution was used to prepare the $[Ag_4(\mathbf{1})](BArF)_4$ / ETH mixture in different proportion.

1:1 mixture of $[Ag_4(\mathbf{1})](BArF)_4$ and ETH

^{1}H NMR (400 MHz, CD_2Cl_2, 298 K) δ (ppm): 8.67 (d, ^3J = 4.9 Hz, 1H, H_6), 8.52 (s, 16H, H_{pyr}), 8.15 (dd, ^3J = 7.7 Hz, 8H, $H_{o\mathit{out}}$), 7.78 (br s, 8H, H_t), 7.75 (br s, 32H, $H_{o\text{-}BArF}$), 7,70 (d, ^3J= 7.7 Hz, 8H, $H_{m\mathit{out}}$), 7.65 – 7.59 (m, 8H, $H_{o\mathit{in}}$), 7.57 (br s, 16H, $H_{p\text{-}BArF\text{-}}$), 7.39 (s, 1H, H_3), 7.33 (d, ^3J = 4.9 Hz, 1H, H_5), 7.20 (br s, 8H, $H_{m\mathit{in}}$), 5.80 (s, 16H, H_{H1}), 4.70 (s, 16H, H_{H2}), 3.78 (s, 16H, H_{H3}), 2.87 (q, ^3J = 7.6 Hz, 2H, H_{CH2}), 1.37 – 1.28 (m, 3H, H_{CH3}), – 3.4 (s, 4H, H_{NH}).

1:2 mixture of $[Ag_4(\mathbf{1})](BArF)_4$ and ETH

^{1}H NMR (400 MHz, CD_2Cl_2, 298 K) δ (ppm): 8.67 (d, ^3J = 4.9 Hz, 2H, H_6), 8.50 (s, 16H, H_{pyr}), 8.08 (d, ^3J = 7.7 Hz, 8H, $H_{o\mathit{out}}$), 7.75 (br s, 32H, $H_{o\text{-}BArF}$), 7.69 (s, 8H, H_t), 7.69 – 7.65 (m, 8H, $H_{m\mathit{out}}$), 7.62 – 7.56 (m, 8H, $H_{o\mathit{in}}$), 7.57 (br s, 16H, $H_{p\text{-}BArF\text{-}}$), 7.39 (s, 2H, H_3), 7.33 (d, ^3J = 4.9 Hz, 2H, H_5), 7.10 – 6.99 (m, 8H, $H_{m\mathit{in}}$), 5.77 (s, 16H, H_1), 4.67 (s, 16H, H_{H2}), 3.74 (s, 16H, H_{H3}), 2.87 (q, ^3J = 7.6 Hz, 4H, H_{CH2}), 1.37 – 1.28 (m, 6H, H_{CH3}), – 3.45 (s, 4H, H_{NH}).

1:3 mixture of $[Ag_4(\mathbf{1})](BArF)_4$ and ETH

^{1}H NMR (400 MHz, CD_2Cl_2, 298 K) δ (ppm): 8.67 (d, ^3J = 4.9 Hz, 2H, H_6), 8.57 (d, ^3J = 5.0 Hz, 1H, $H_{6'}$), 8.50 (s, 16H, H_{pyr}), 8.07 (d, ^3J = 7.7 Hz, 8H, $H_{o\mathit{out}}$), 7.75 (br s, 32H, $H_{o\text{-}BArF}$), 7.67 (s, 8H, H_t), 7.67 – 7.65 (m, 8H, $H_{m\mathit{out}}$), 7.62 – 7.56 (m, 8H, $H_{o\mathit{in}}$), 7.57 (br s, 16H, $H_{p\text{-}BArF}$), 7.51 (s, 1H, $H_{3'}$), 7.42 (d, ^3J = 5.0 Hz, 1H, $H_{5'}$), 7.39 (s, 2H, H_5), 7.33 (d, ^3J = 4.9 Hz, 2H, H_5), 7.04 (d, ^3J = 7.9 Hz, 8H, $H_{m\mathit{in}}$), 5.77 (s, 16H, H_{H1}), 4.67 (s, 16H, H_{H2}), 3.73 (s, 16H, H_{H3}), 2.90 – 2.81 (m, 6H, $H_{CH2,\ CH2'}$), 1.36 – 1.28 (m, 9H, H_{CH3}), – 3.45 (s, 4H, H_{NH}).

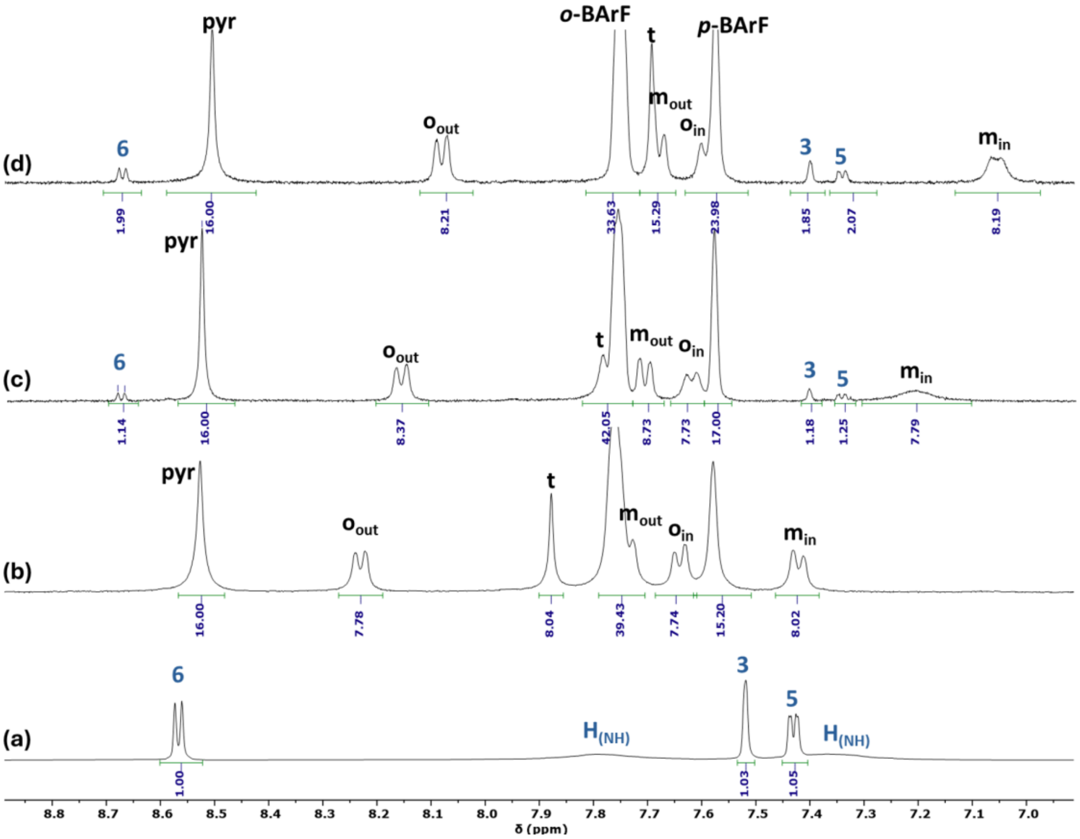

Fig. S14A: Selected regions of the ^{1}H NMR (400 MHz, CD_2Cl_2, 298 K, 8.9 ppm - 6.9 ppm) spectra of ETH (a), $[Ag_4(\mathbf{1})](BArF)_4$ (b) and $[Ag_4(\mathbf{1})](BArF)_4$ with incremental amounts of ETH: 1 equivalent (c), 2 equivalents (d).

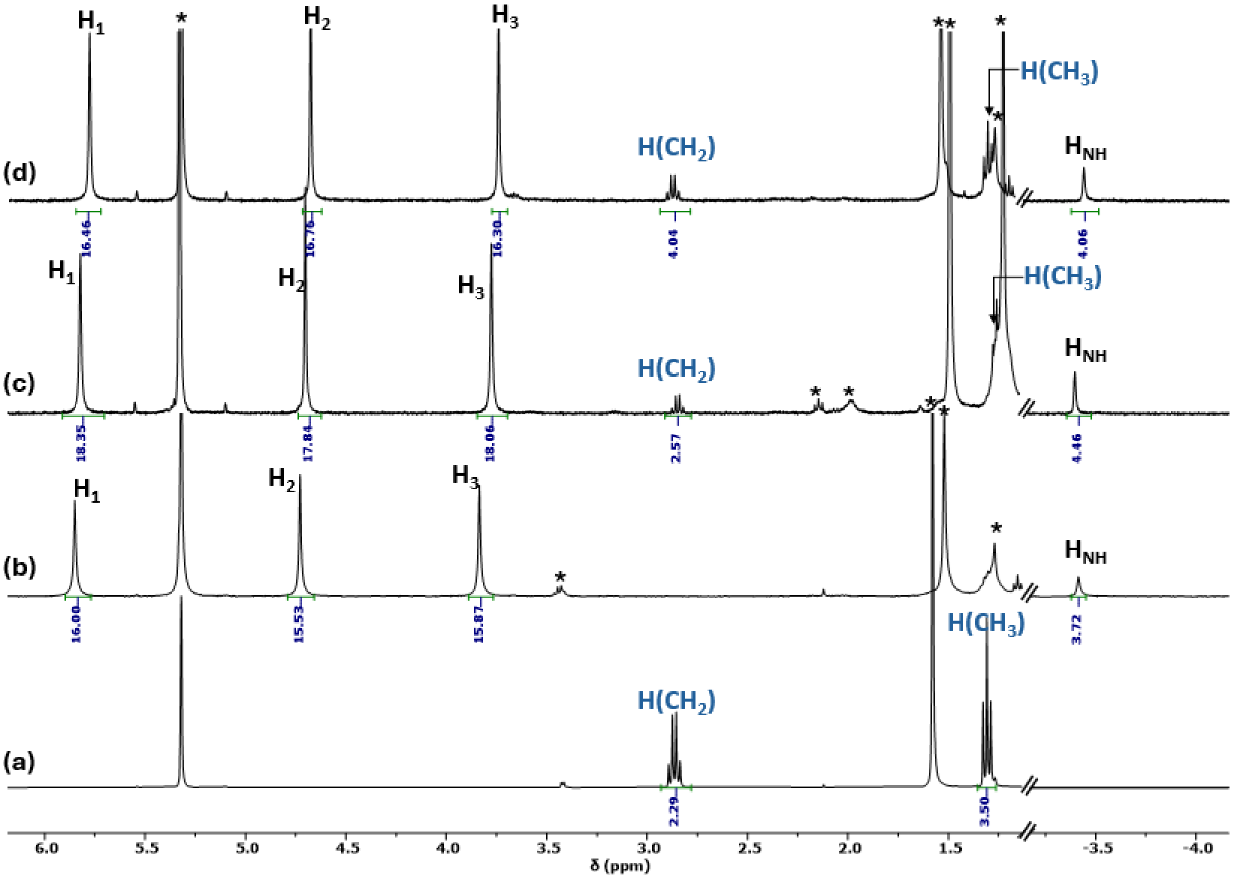

Fig. S14B: Selected regions of the ^{1}H NMR (400 MHz, CD_2Cl_2, 298 K, 6.8 ppm - −4.0 ppm) spectra of ETH (a), [Ag_4(**1**)]$(BArF)_4$ (b) and [Ag_4(**1**)]$(BArF)_4$ with incremental amounts of ETH: 1 equivalent (c), 2 equivalents (d). *: residual solvents or grease.

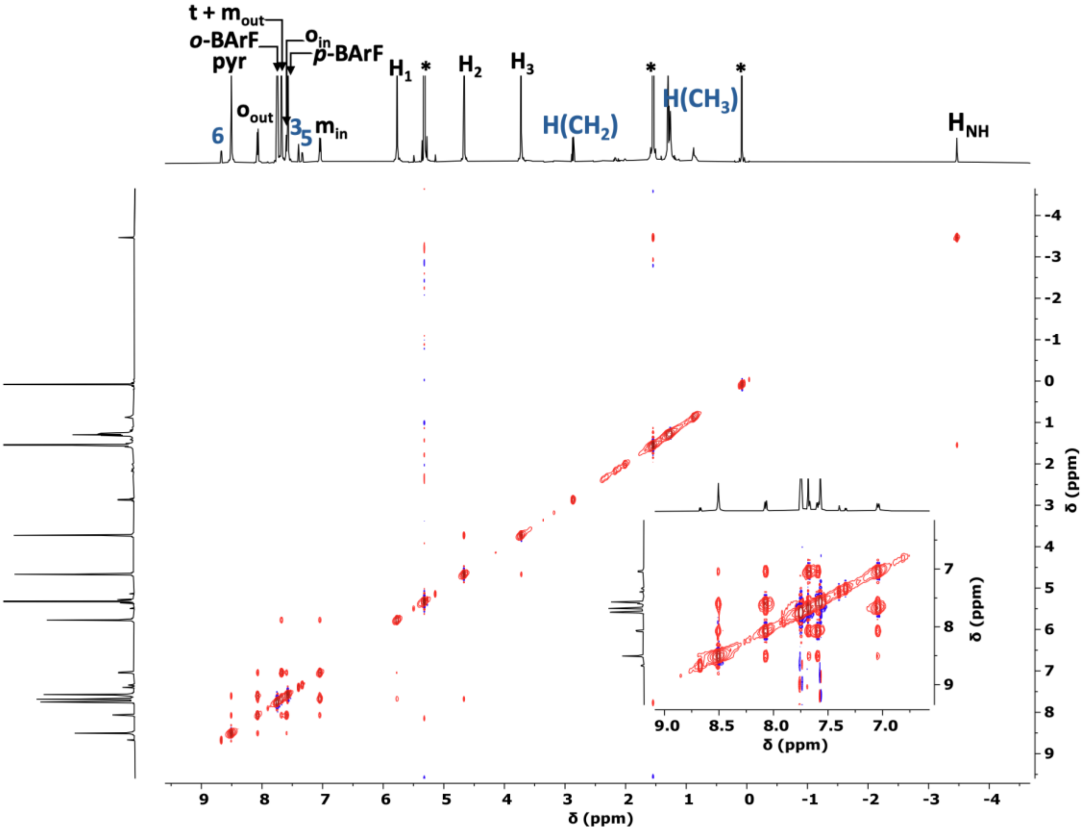

Fig. S15: NOESY NMR (500 MHz, CD_2Cl_2, 298 K) spectrum of the 1:2 mixture of $[Ag_4(\mathbf{1})](BArF)_4$ and ETH . *: residual solvents.

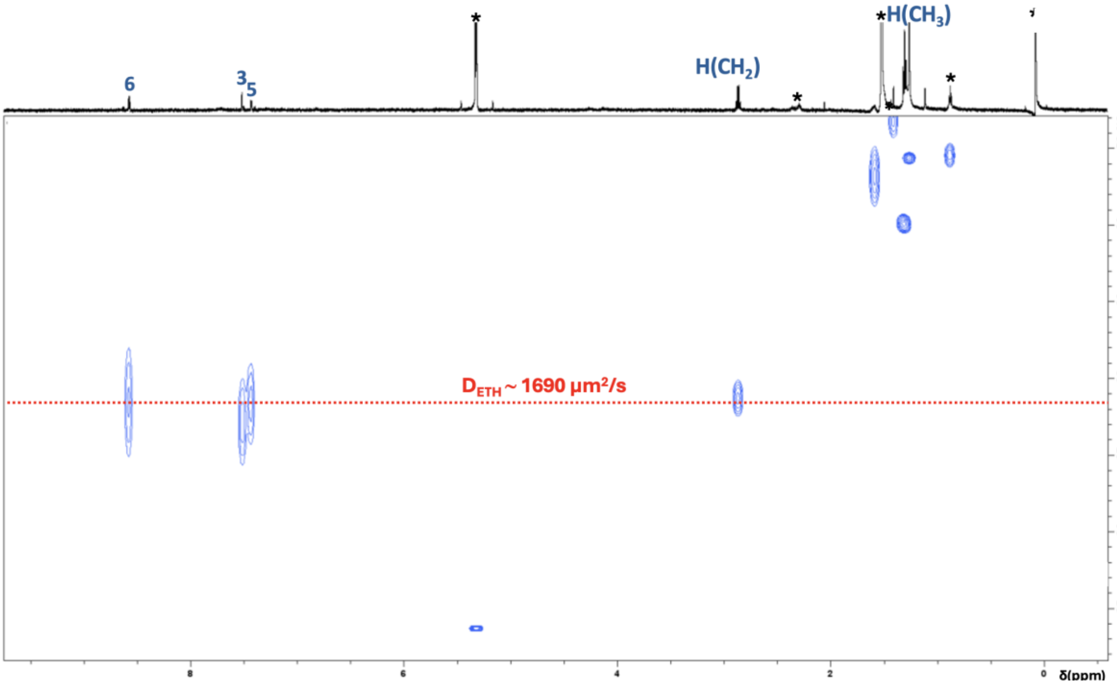

Fig. S16: DOSY NMR (600 MHz, CD_2Cl_2, 298 K) spectrum of ETH. *: residual solvents or grease.

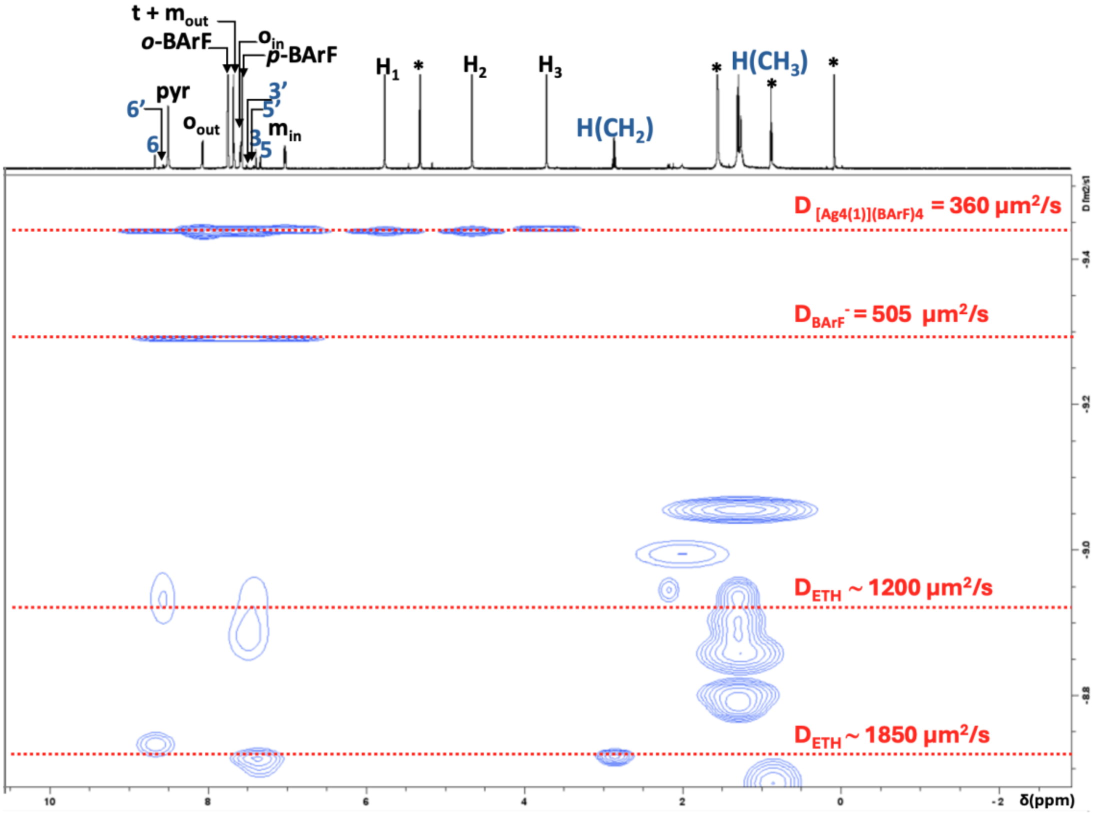

Fig. S17: DOSY NMR (600 MHz, CD_2Cl_2, 298 K) spectrum of the 1:2 mixture of [Ag_4(**1**)]$(BArF)_4$ and ETH. *: residual solvents or grease.

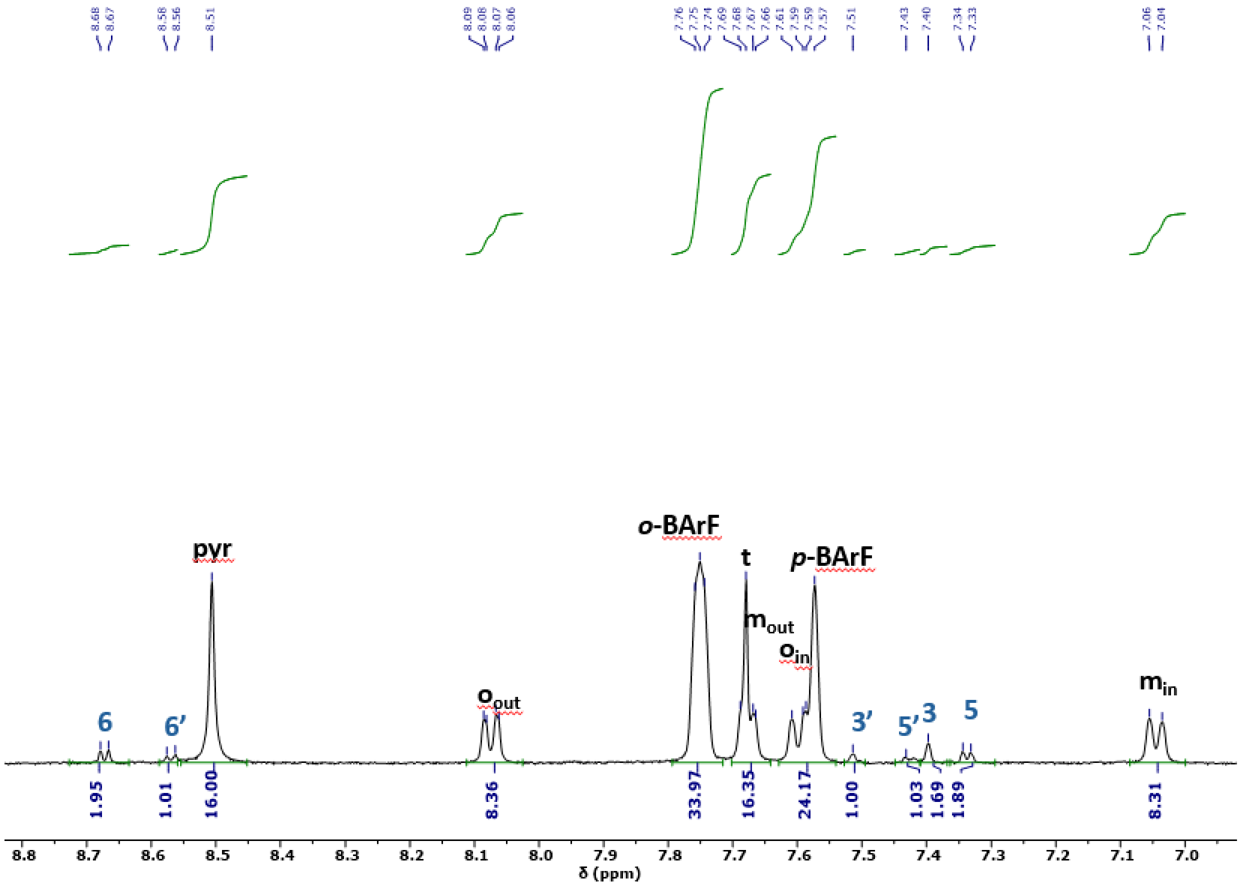

Fig. S18A: Selected region of the ^{1}H NMR (400 MHz, CD_2Cl_2, 298 K, 8.8 ppm - 7.0 ppm) spectrum of the 1:3 mixture of $[Ag_4(\mathbf{1})](BArF)_4$ and ETH.

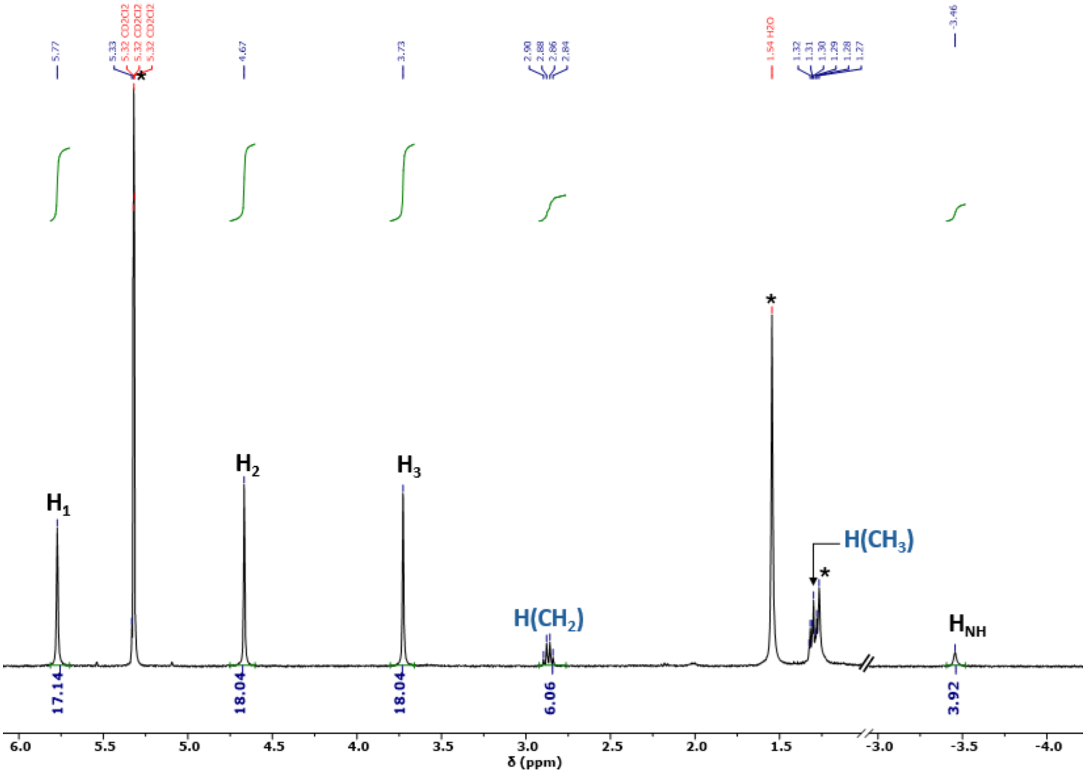

Fig. S18B: Selected region of the ^{1}H NMR (400 MHz, CD_2Cl_2, 298 K, 6.0 ppm - −4.0 ppm) spectrum of the 1:3 mixture of $[Ag_4(\mathbf{1})](BArF)_4$ and ETH.

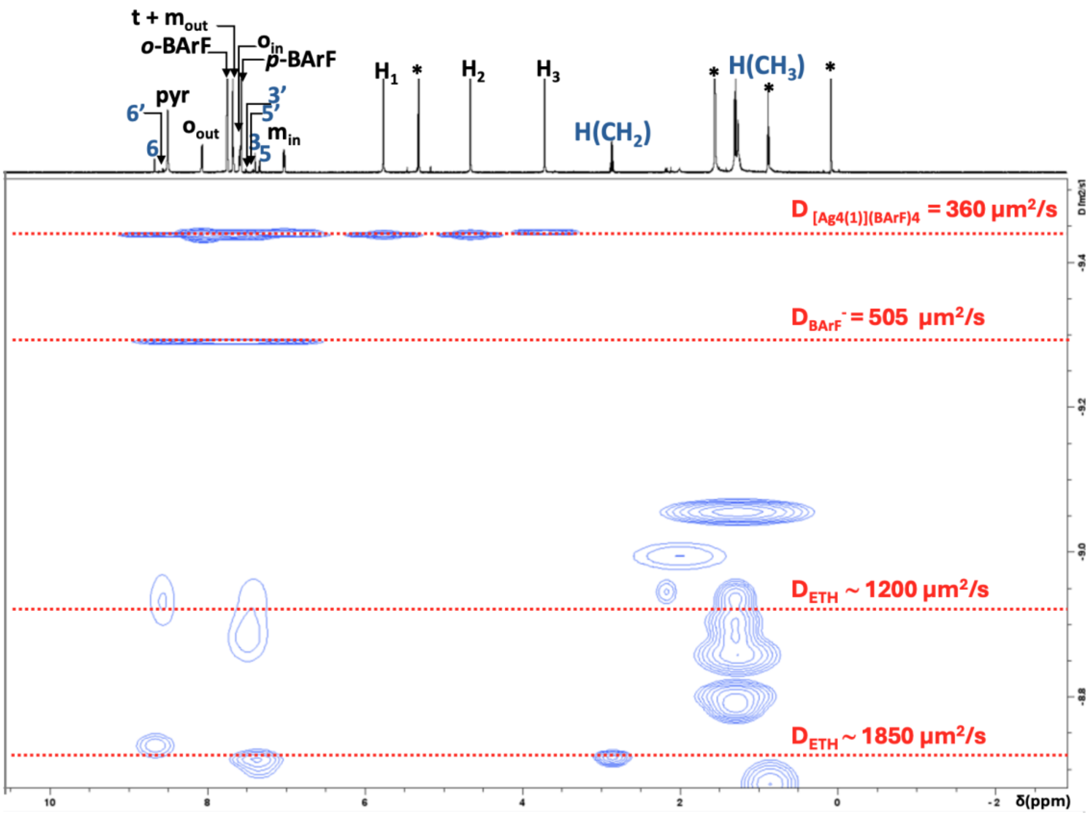

Fig. S19: DOSY NMR (600 MHz, CD_2Cl_2, 298 K) spectrum of the 1:3 mixture of $[Ag_4(\mathbf{1})](BArF)_4$ and ETH.*: residual solvents.

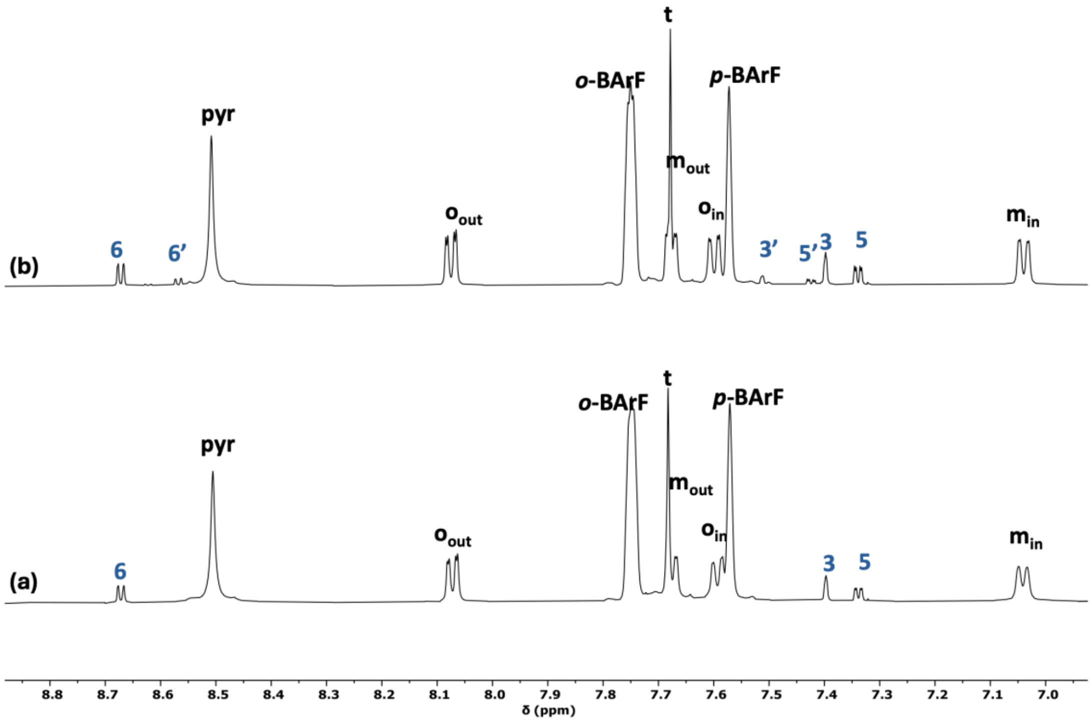

Fig. S20A: Selected regions of the ^1H NMR (500 MHz, CD_2Cl_2, 298 K, 8.8 ppm – 7.0 ppm) spectra after 10 days of $[Ag_4(\mathbf{1})](BArF)_4$ with incremental amounts of ETH: 2 equivalents (a), 3 equivalents (b).

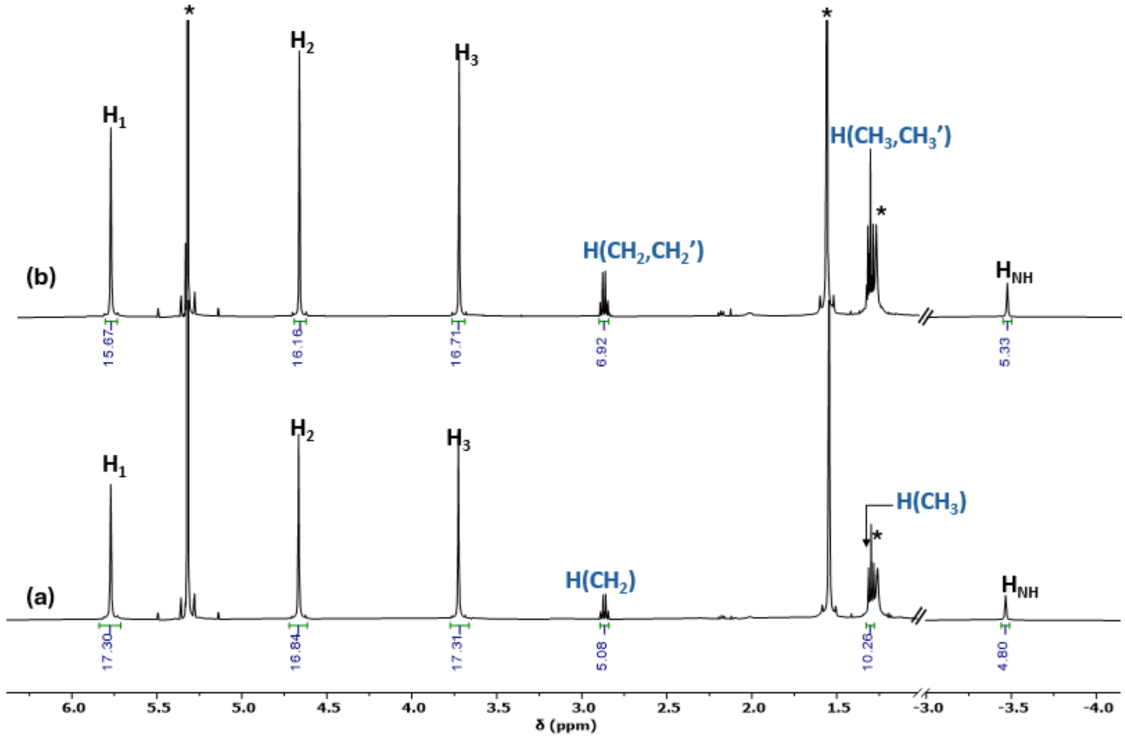

Fig. S20B: Selected regions of the ^{1}H NMR (500 MHz, CD_2Cl_2, 298 K, 6.0 ppm – -4.0 ppm) spectra after 10 days of [Ag_4(**1**)]$(BArF)_4$ with incremental amounts of ETH: 2 equivalents (a), 3 equivalents (b). *: residual solvents.

3.2 NMR studies of ETH interaction with [Na₄(1)](BArF)₄

1:1 mixture of [Na_4(**1**)]$(BArF)_4$ and ETH

To a solution of cage [Na_4(**1**)]$(BArF)_4$ (1.71 mg, 0.3 µmol, 1 equiv.) in CH_2Cl_2 was added ETH (100 µL of a 3 mM solution in CH_2Cl_2/MeOH (9:1), 7.48 µmol, 1 equiv.) and K_2CO_3 (4 mg, 22 µmol). The mixture was sonicated for 2 min and evaporated *in vacuo*. The residue was dissolved in 0.6 mL of CD_2Cl_2.

^{1}H NMR (400 MHz, CD_2Cl_2, 298 K) δ (ppm): 8.57 (d, ^3J = 4.9 Hz, 2H, H_6), 8.48 (s, 16H, H_{pyr}), 8.06 (d, ^3J = 7.7 Hz, 8H, $H_{o\mathit{out}}$), 7.86 – 7.70 (m, 42H, $H_{o\text{-}BArF,\ t,\ NH2}$), 7,70 – 7.67 (d, ^3J = 7.7 Hz, 8H, $H_{m\mathit{out}}$), 7,62 – 7.57 (m, 8H, $H_{o\mathit{in}}$), 7.57 (br s, 16H, $H_{p\text{-}BArF\text{-}}$), 7.51 (s, 1H, H_3), 7.33 (d, ^3J = 4.9 Hz, 1H, H_5), 7.15 (d, ^3J = 7.7 Hz, 8H, $H_{m\mathit{in}}$), 5.78 (s, 16H, H_{H1}), 4.74 (s, 16H, H_{H2}), 3.82 (s, 16H, H_{H3}), 2.86 (q, ^3J = 7.6 Hz, 2H, H_{CH2}), 1.37 – 1.28 (m, 3H, H_{CH3}), – 3.48 (s, 4H, H_{NH}).

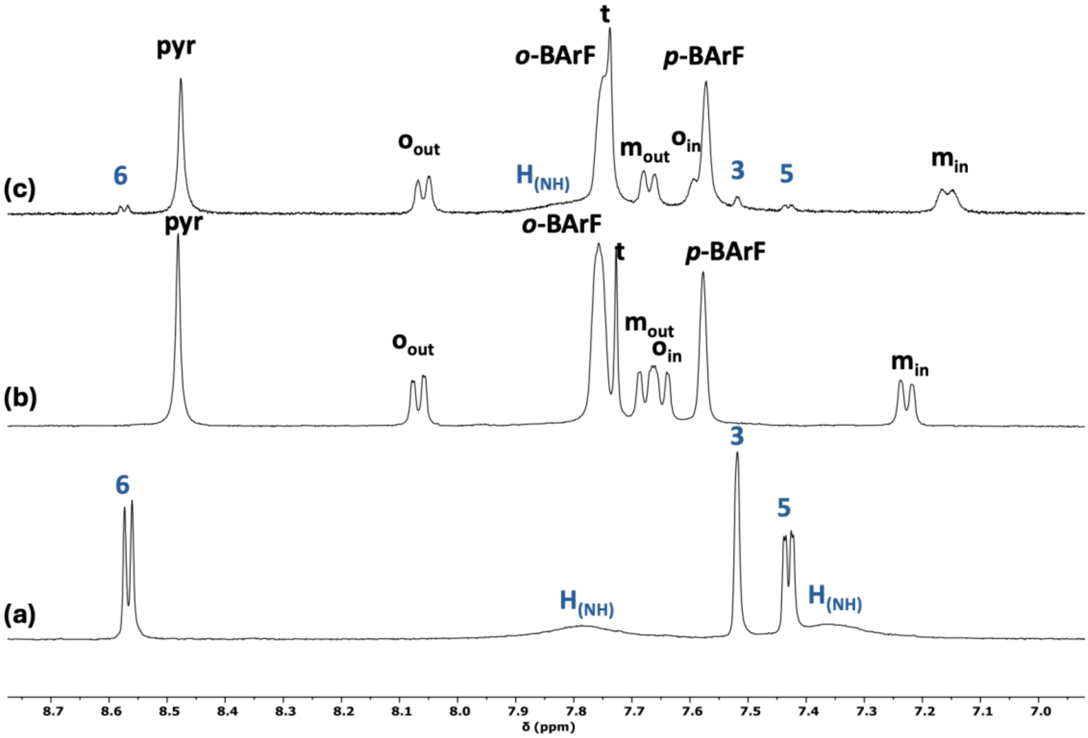

Fig. S21A: Selected regions of the ^{1}H NMR (400 MHz, CD_2Cl_2, 298 K, 8.7 ppm – 7.0 ppm) spectra of ETH (a), $[Na_4(\mathbf{1})](BArF)_4$ (b) and $[Na_4(\mathbf{1})](BArF)_4$ with 1 equivalent of ETH: (c).

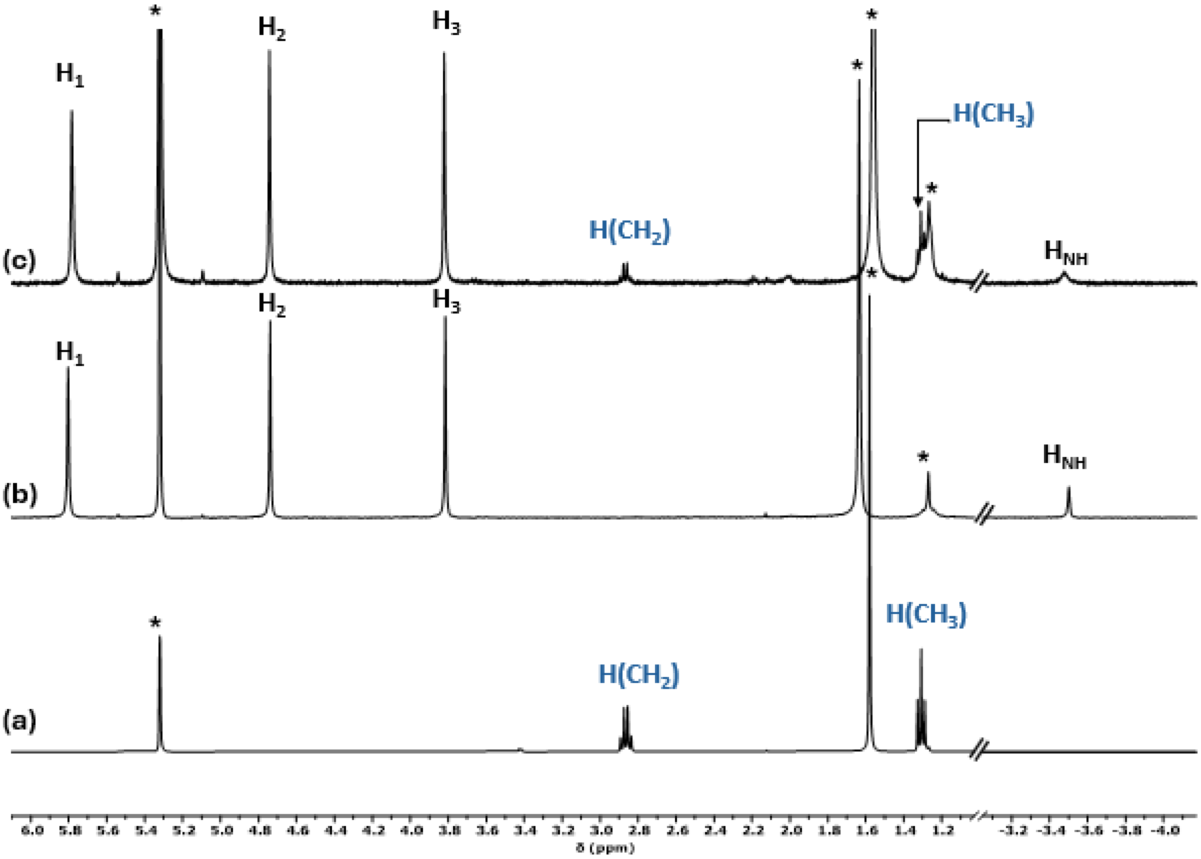

Fig. S21B: Selected regions of the ^{1}H NMR (400 MHz, CD_2Cl_2, 298 K, 6.0 ppm – -4.0 ppm) spectra of ETH (a), $[Na_4(\mathbf{1})](BArF)_4$ (b) and $[Na_4(\mathbf{1})](BArF)_4$ with 1 equivalent of ETH: (c). *: residual solvents or grease.

4. Computational analysis

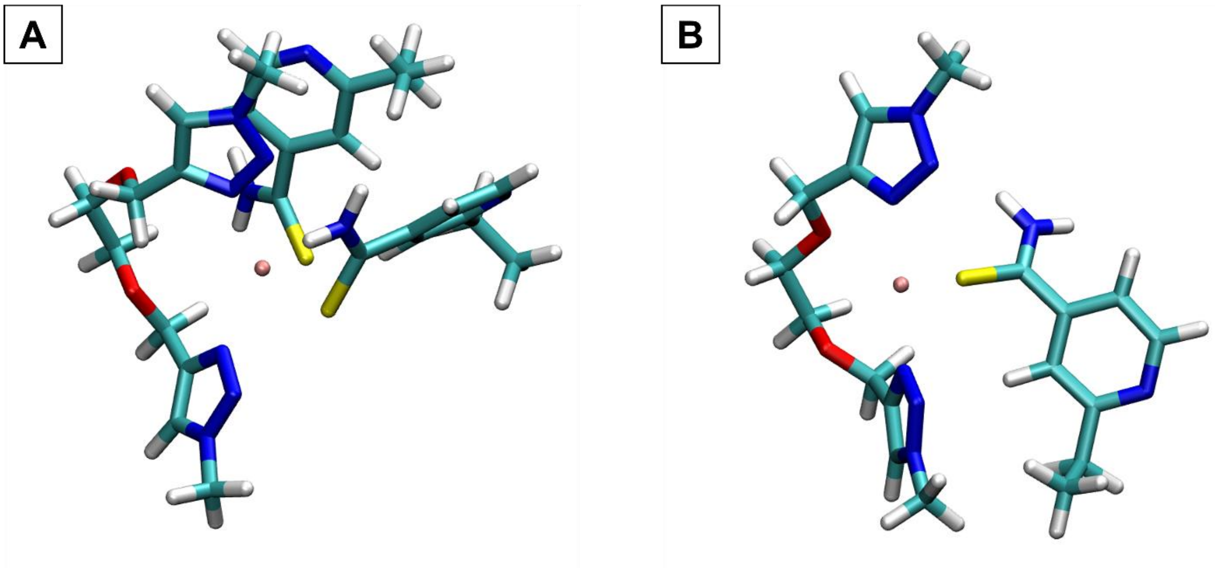

Fig. S22: (A) Optimized structure with two ETH molecules coordinating the same Ag(I) ion. (B) Optimized structure with one ETH molecule coordinating an Ag(I) ion.